Acta Geotechnica. May 2014.

Construction, management and maintenance of embankments used for road and rail infrastructure: implications of weather induced pore water pressures

Stephanie Glendinning[1], Paul Hughes[1], Peter Helm[1], Jonathan Chambers[2], Joao Mendes[3], David Gunn[2], Paul Wilkinson[2] and Sebastien Uhlemann[4]

(1) School of Civil Engineering and Geosciences, Newcastle University, Drummond Building, Newcastle upon Tyne, NE1 7RU, UK
(2) British Geological Survey, Keyworth, UK
(3) The School of Engineering, The University of Newcastle, Newcastle, Australia
(4) ETH Zürich, Department of Earth Sciences, Institute of Geophysics, Zürich, Switzerland

Abstract

Understanding the age and construction quality of embankments used for road and rail infrastructure is critical in the effective management and maintenance of our transport networks, worth £billions to the UK economy. This paper presents for the first time results from full-scale, carefully controlled experiments on a unique model embankment conducted over the 4-year period between 2008 and 2011. It combines point location and spatially distributed measurements of pore water pressures and water content with outputs from hydrological modelling to draw conclusions of significance to both ongoing research in this field and to the asset management practices of infrastructure owners. For researchers, the paper highlights the crucial importance of transient permeability and soil water retention behaviour of fill materials in controlling the magnitude and distribution of pore water pressure in response to climate and weather events. For practitioners, the work demonstrates that there are significant differences in pore water pressure behaviour across the embankment, which is influenced by construction-related issues such as compaction level, aspect and presence of a granular capping material. Permeability was also observed to vary across the embankment both spatially and with depth, being dependent on degree of saturation and macroscale effects, particularly within a 'near surface zone'. It is proposed that this 'near surface zone' has a critical effect on embankment stability and should be the focus of both ongoing scientific research and inspection and monitoring as encompassed by asset management regimes.

Keywords

Embankments - Field monitoring - Partial saturation - Permeability - Pore pressures - Suction

Notes

This is the version of the manuscript accepted by the journal including changes made following reviewers comments. The final publication is available at Springer via:

http://dx.doi.org/10.1007/s11440-014-0324-1.

The final publication is available at Springer via
http://dx.doi.org/10.1007/s11440-014-0324-1

1. Introduction

Infrastructure slopes (including embankments and cuttings) represent approximately one third of the total asset value of the UK's transport infrastructure [1]. In common with most of the developed world, this infrastructure is ageing and much of it was constructed before the development of modern soil mechanics theories; deformation and failure are therefore common [2]. Failures on these slopes have the potential to close sections of transport infrastructure causing delays and, in extreme cases, pose a risk to the lives of transport users. The cost of emergency repair is estimated to be 10 times that of planned maintenance [3]. Therefore, improvement of our understanding of the processes of ageing and deterioration of embankments to the degree where we can advance construction management and maintenance systems will have significant cost and safety advantages for global infrastructure.

Anderson et al. [4], Ridley et al. [5], Nyambayo et al. [6], Smethurst et al. [7], Hughes et al. [8] and Glendinning et al. [3, 9] have all identified the role of water (pore water pressures), vegetation and permeability as important parameters in governing the stability of infrastructure slopes of all ages. Pore water pressures are known to vary seasonally and in response to climatic events. These climatically driven seasonally varying effects on the water balance are significant because the stress changes, they cause act to apply fluctuating loads to the fill material within embankments. The suctions present within the partially saturated portions of a slope will also alter the effective shear strength of the fill and cause variations in hydraulic conductivity dependent on the degree of saturation. Deformations, caused by volumetric changes, shear strains and tension cracking also impact on the pore water pressure and permeability of engineered fill through changes to the micro- and macroscale fabric of the material.

The impact of these variations has been widely demonstrated in the literature where fluctuations in embankment pore water pressures due to seasonal and climatic variations are seen to have a significant impact on infrastructure slope stability [2,7,10,11,12,13,14,15,16]. Further evidence of this is demonstrated by the significant effort expended on numerical modelling of embankment stability as influenced by seasonal fluctuations in pore water pressure which has been undertaken by a number of authors including Kovacevic et al. [17], Nyambayo et al. [6], O'Brien [18], Scott et al. [19] and Rouainia et al. [20]. Furthermore, there have been numerous studies of the effects of wetting and drying on the stability of slopes; for example, the investigation of triggering mechanisms for landslides in natural slopes [21] and in engineered slopes [22].

The aim of the research presented in this paper was to investigate the relative influence of long- and short-duration weather events on the fluctuations of pore water pressure within a unique full-scale model glacial till clay embankment representative of UK transport infrastructure. The work has, for the first time, integrated point location and spatially distributed measurements of pore water pressures and water content with outputs from hydrological modelling of carefully controlled experiments in which artificially induced rainfall is used to simulate storm events. The particular objective of the work was to examine the results of the experiments in terms of construction-related effects such as degree of compaction, slope aspect and crest capping and thus comment on the implications for monitoring, modelling and maintenance of road and rail embankments.

2. Test embankment construction and characterisation

A full-scale test embankment was constructed in 2005, which was 90 m long, 6 m high, 29 m wide and with a 5-m crest and 1 in 2 slopes, orientated along its length in an east to west direction. This geometry was chosen so as to be representative of typical UK infrastructure embankments based on the report published by Perry et al. [1]

The embankment is located at Nafferton Farm, Stocksfield, Northumberland (Ordinance Survey grid Reference NZ 064 657). Foundation conditions were stiff to hard glacial till with an in situ permeability ranging from 1×10^{-10} to 1×10^{-12} m/s. Further details of design, construction process, instrumentation and materials testing are provided in Hughes et al. [8].

The embankment was constructed in four 18-m-long sections: the two innermost sections (panels B and C, 36 m long in total, Figure 1) were constructed according to UK Highways Agency specifications (termed the 'well compacted panels') and simulate new-build highway embankments; the two outermost sections (panels A and D, Figure 1) were built to represent poorly constructed/heterogeneous rail embankments. This was achieved by placing fill in 1.3 m lifts with minimum tracking by site plant. Thus, the degree of compaction was reduced, and 'controlled' heterogeneities were incorporated into the structure of the fill. A 0.5-m layer of coarse capping material of type 6F5 [23] composed of Basalt was also placed along the crest of the embankment.

The final publication is available at Springer via
http://dx.doi.org/10.1007/s11440-014-0324-1

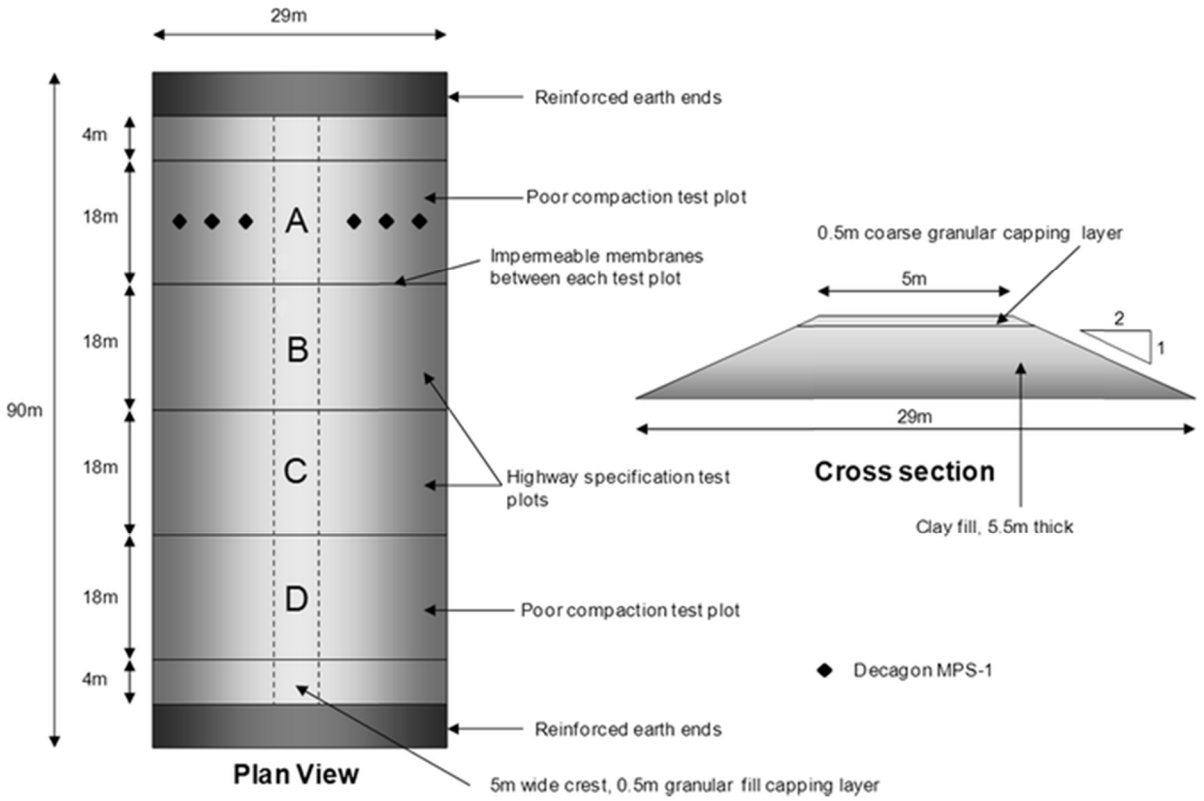

Figure 1: Embankment plan view and cross section

Impermeable membranes were installed during construction between the panels to prevent any hydraulic connectivity between each section. The slopes were seeded immediately after construction with grassland seeds typical of the North East of England, and other plant species were allowed to colonise the embankment naturally.

A range of characterisation tests have been performed on the embankment fill material; this paper focuses on density, permeability and soil water retention which are crucial to the understanding of hydrological processes, and hence, the pore water pressure changes resulting from rainfall infiltration.

The fill material used in the construction of the embankment was a locally sourced glacial till. Its Atterberg limits, tested in accordance with BS 1377 [24], were 45 and 24 % for liquid and plastic limits, respectively (average values calculated from 12 No. tests), which classifies the fill material to be of intermediate plasticity. The results of quantitative XRD analyses on the sub 2 µm fraction of the embankment fill material suggests that the clay mineral assemblages are generally similar and composed of variable amounts of illite/smectite (ranging from 42 to 54 %, with a mean of 49 %), chlorite/smectite (3–7 % range, mean 5 %), illite (16–26 % range, mean 19 %) and kaolinite (23–31 % range, mean 26 %). In all cases, the separated sub 2 µm fractions also contain small quantities of quartz and lepidocrocite (γ-FeOOH).

The final publication is available at Springer via
http://dx.doi.org/10.1007/s11440-014-0324-1

Laboratory assessment of compaction characteristics of the fill were performed according to BS1377 and are illustrated in Figure 2. Using normal Proctor (light) compaction, the maximum dry density of the embankment fill was measured to be 1.71 Mg/m^3 at an optimum water content (W_{opt}) of 15.5 % and the modified (heavy) compaction maximum dry density was measured to be 1.80 Mg/m^3 at a W_{opt} of 13 %.

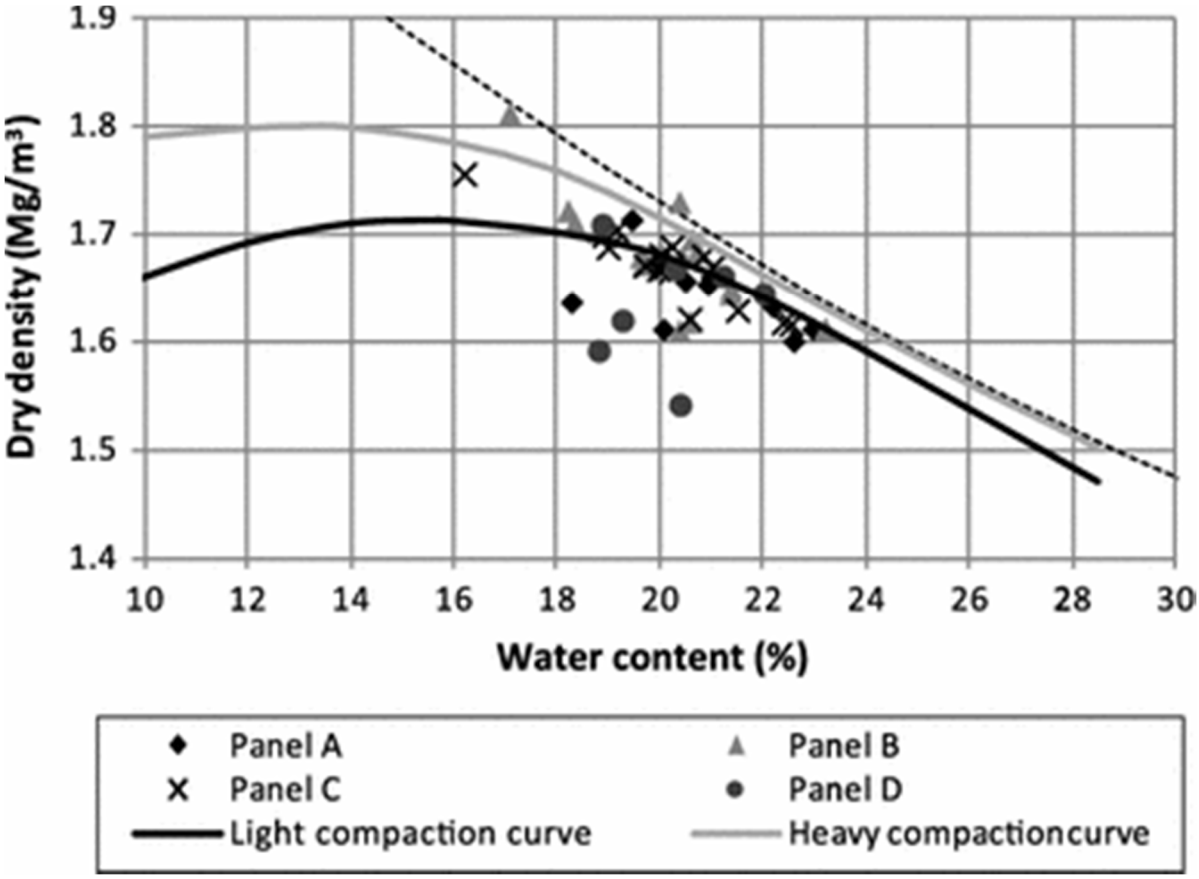

Figure 2: Compaction curves versus field measurements (panels A and D—poorly compacted; B and C—Well compacted)

Throughout construction, core cutter density samples were taken after each layer was compacted to build up a detailed record of the initial conditions of the embankment. The densities achieved during construction for both well- and poorly compacted panels have been plotted onto the laboratory determined compaction curves shown in Figure 2; a section showing variation with depth is shown in Figure 3a and void ratio variation with depth in Figure 3b. The majority of the measured values were close to the light compaction curve with density values above the optimum moisture content. The average density of the well-compacted panels was higher (1.7 Mg/m^3) than the average density of the poorly compacted panel (1.6 Mg/m^3). Although similar in density, the average percentage of air voids present in the poorly compacted panels was higher (6.0 %) than the average air voids in the well-compacted panel (3.2 %). Some densities recorded in panels A and D vary significantly from the mean,

The final publication is available at Springer via
http://dx.doi.org/10.1007/s11440-014-0324-1

the variation being attributed to variations in the 'light' compaction applied to these panels. These variations in density will clearly affect the porosity which in turn affects permeability and the soil water retention properties of the material.

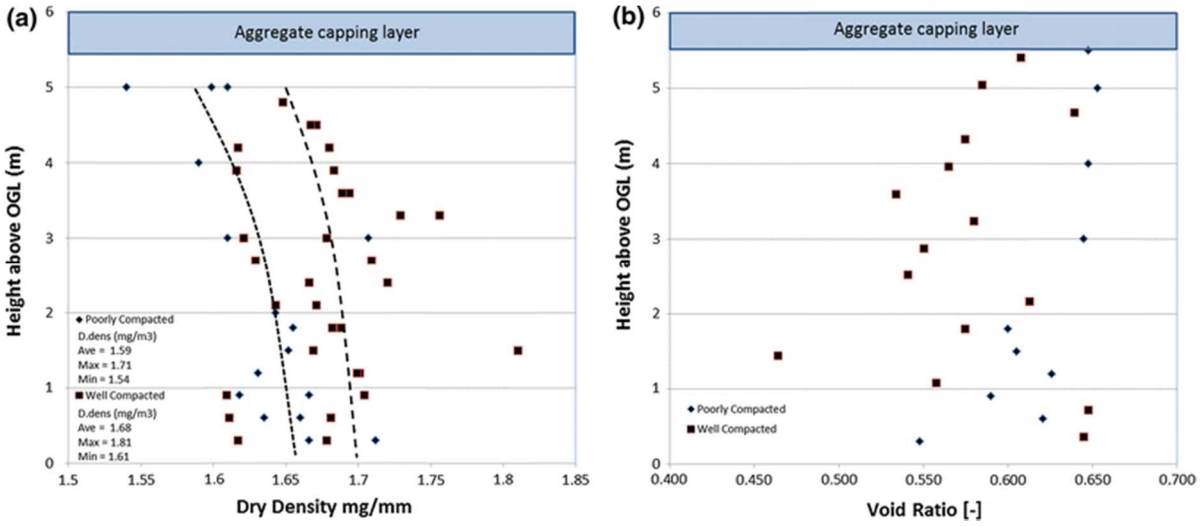

Figure 3: (a) In situ, dry density of well- and poorly compacted panels immediately after construction. (b) In situ, void ratio of well and poorly compacted panels immediately after construction

Soil water retention curves (SWRC) were obtained from specimens that were initially prepared using normal Proctor (light) compaction at a water content of 25 % to develop a degree of saturation close to 100 % and then dried out in stages. At each stage, specimens were tested for suction and volumetric and gravimetric water contents. Two different techniques were used to measure suctions: the first used the in-contact filter paper methodology presented by Bulut et al. [25], which determines suction indirectly, based on the water content of a filter paper placed in contact with the sample. In this case, the calibration curve presented by Leong et al. [26] was used to determine values of suction. The second technique was based on high-capacity suction probes, which can measure suction directly [4, 27]. For this work, DU-WF high-capacity suction probes were used, which have a measuring range of more than 2 MPa [26]. The SWRC can be seen in Figure 4a following the drying paths and shows that good agreement was reached between the two techniques. The residual water content was found to be 4 %. The relationship between matric suction and the degree of saturation is shown in Figure 4b where the high air-entry value of the fill material was determined to be close to 600 kPa.

Two years after construction, core samples were retrieved from embankment panels A (poorly compacted) and B (well compacted). Specimens were prepared from the cores taken at 1 m depth, and matric suction measured using the high-capacity suction probe technique (using a drying stage methodology on specimens dried from their in situ water content) and plotted against water content.

Results of these tests are shown in Figure 4c. The resulting suctions in specimens taken from the well-compacted panel fit the primary drying curve established in previous laboratory experiments closely; specimens prepared from the poorly compacted panel have produced lower values of suction for the same value of water content than those taken from the well-compacted panel. These SWRCs are likely to be scanning (wetting) curves due to the initial water contents and should only be considered in qualitative terms since the test was performed under no confining pressure, a factor that differs from the in situ situation.

The final publication is available at Springer via
http://dx.doi.org/10.1007/s11440-014-0324-1

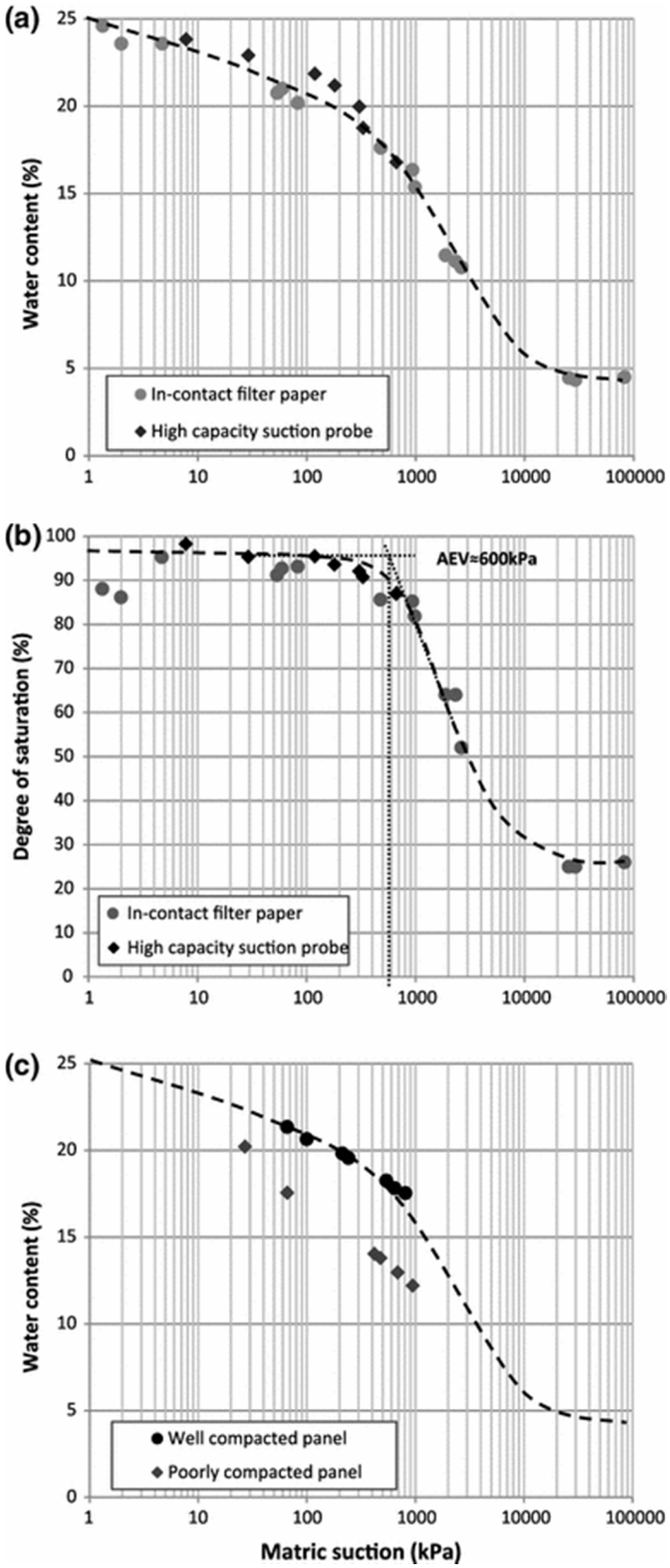

Figure 4: SWRC. (a) Gravimetric water content versus matric suction, obtained from compacted specimens by in-contact filter paper and high-capacity suction probe. (b) Degree of saturation versus matric suction obtained from compacted specimens by in-contact filter paper and high-capacity suction probe. (c) SWRCs obtained from specimens of the first metre of the well- and poorly compacted panels compared with the SWRC from laboratory compacted specimens

The final publication is available at Springer via
http://dx.doi.org/10.1007/s11440-014-0324-1

3. Full-scale experimentation: methodology

Extensive arrays of monitoring devices were installed throughout the embankment to observe the impact of cyclic climate variation and weather events produced by both natural and artificially imposed rainfall. Extensometer data from the section under consideration show primary settlement were complete prior to the study period (shown in Figure 5)—inclinometer data also show no displacements higher than 5 mm—within the error margin of the instruments. Therefore, this paper focuses on pore water pressure responses driven by weather events alone with any effect caused by volumetric changes due to consolidation and shear strains being discounted.

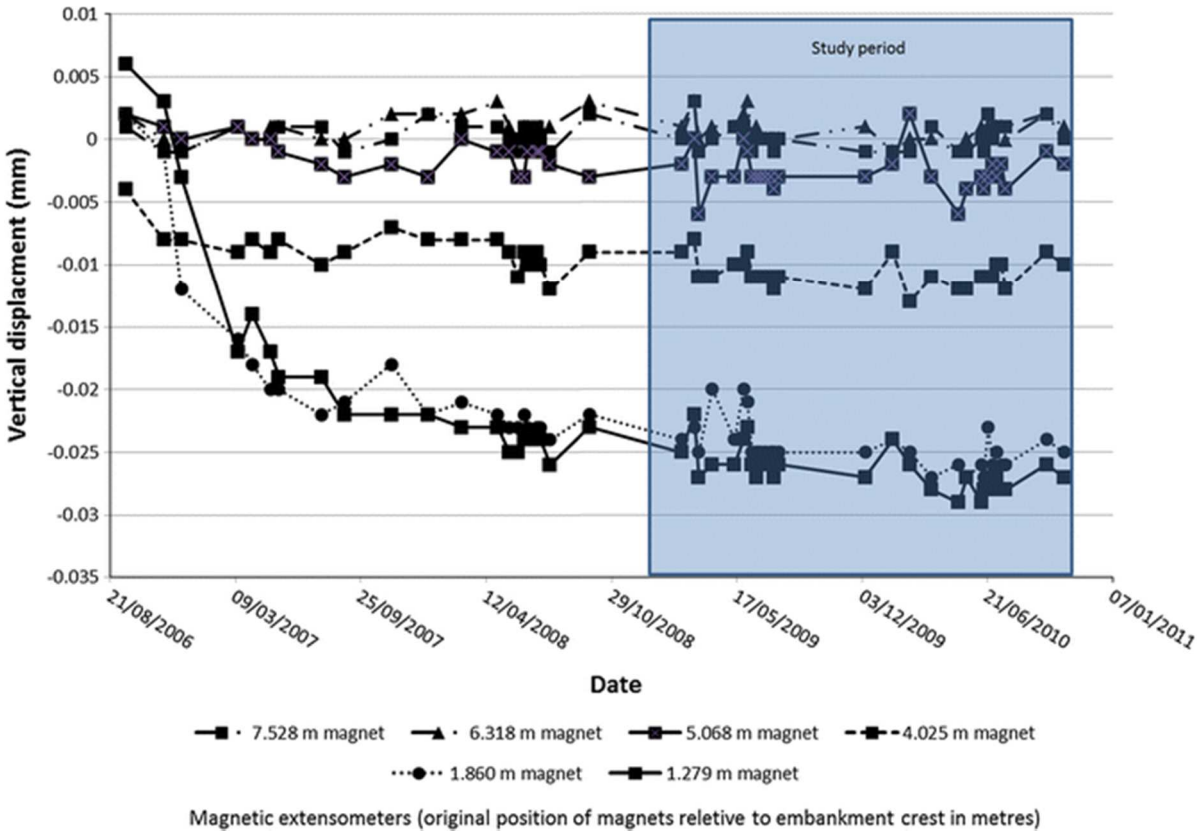

Figure 5: Settlement recorded using magnetic extensometers in poorly compacted panel A

A computer controlled sprinkler system was installed over the embankment covering the poorly compacted panel A and well-compacted panel B to increase natural precipitation levels and simulate storm events. The system was used to add an even distribution (ensured using cup tests) of water to the surface at a rate of 33 mm per day from sprinklers mounted at a height of 1.5 m above the ground surface. This system has been used for extensive periods during the summers of 2008, 2009 and 2010. The observed changes over the natural precipitation have been recorded hourly by three independent weather stations. These weather stations monitor precipitation, incident shortwave solar radiation, air temperature, wind direction and speed. One of the weather stations was placed 300 m east of the

The final publication is available at Springer via
http://dx.doi.org/10.1007/s11440-014-0324-1

embankment and provides benchmark data for the site, whilst two 'mini' weather stations, placed directly onto the slopes of the embankment, monitor the changes imposed by the simulated precipitation system.

Effective measurement of run-off, representative of a whole panel, has not been achieved due to variability caused by surface features, including vegetation, cracking and above-ground instrumentation.

It was necessary to develop an understanding of the water balance within the embankment in order to effectively interpret the pore water pressure data. This required an understanding of the likely water movements, which are controlled by the permeability of the soil mass. Therefore, the results of permeability testing are presented, followed by the water balance determination and then the pore water pressure results plotted as a function of effective recharge. In addition, electrical resistivity tomography (ERT) is used to determine the spatial distribution of moisture content to complement the point sensor-derived monitoring results.

3.1 Permeability testing

A value for permeability which is representative of a clay fill mass is notoriously difficult to determine. Therefore, a combination of both carefully controlled laboratory tests on specimens prepared from field samples and, in situ, field measurements was undertaken.

Constant head permeability tests (BS1377-5 [28]) were performed on specimens prepared from undisturbed samples recovered post construction from 2 m beneath the crest of the embankment using U100 sampling equipment. Permeability was found to be 8.8×10^{-11} m/s in the well-compacted panels, whereas it increased to 1.6×10^{-10} m/s in the poorly compacted panels [29].

Field testing of permeability has also been carried out extensively across the embankment between depths of 0.3 m and 1.4 m. In situ permeability was determined using a Guelph permeameter, a device designed for field conditions, based on the principle of the falling head test [30]. The Guelph Permeameter measures permeability based on steady state infiltration that occurs once the soil has wetted. However, unlike the laboratory analysis, this type of test is able to account for the effects of macro- and microscale cracking, preferential flow along roots and zones or peds of soil that have not fully saturated.

The final publication is available at Springer via
http://dx.doi.org/10.1007/s11440-014-0324-1

3.2 Water balance determination

The effective groundwater recharge was required in order to determine the effect of weather events on the pore water pressure changes within the embankment. Hence, a detailed appraisal of the water balance within the embankment was carried out. According to Smethurst et al. [7] the dominant parameters affecting the water balance on engineered slopes are rainfall (P), run-off (Q) and evapotranspiration (ET).

These parameters can be used to estimate the effective groundwater recharge (R_e) due to meteorological variables whereby:

$$R_e = P - (ET + Q) \quad (1)$$

The effective recharge terms above can be considered among the surface components of the water balance equation [31]:

$$(P - Q \pm \Delta S_{Sur}) - ET \pm \Delta S_{Soil} - D \approx 0 \quad (2)$$

Where ΔS_{Soil} is the change in ground storage of moisture, ΔS_{Sur} is surface storage (ponding) and D is deep percolation below the level of the rooting zone.

Precipitation (P) was measured on site at meteorological stations on the shoulders of the slope. The ground storage term in this case is equivalent to the measured soil moisture content which was also measured on site.

As direct measurements of evapotranspiration (ET), surface storage (ΔS_{Sur}) and run-off (Q) could not be made, it was necessary to estimate these values by indirect means. This estimate was based on modelling of the site numerically using the finite difference hydrological modelling code SHETRAN which is capable of modelling fully and partially saturated flow behaviour [32]. The assumptions related to the derivation of these parameters are described in more detail below.

The evapotranspiration at the site was derived from the potential evapotranspiration (PET) rate (E), which was calculated for the site using SHETRAN which uses the Penmann-Monteith equation [33]:

$$E = \lambda \frac{\Delta(R_N + G) + \rho_a C_P[(e_s - e_a)/r_a]}{\Delta + \gamma[(r_a - r_s)/r_a]} \quad (3)$$

The final publication is available at Springer via
http://dx.doi.org/10.1007/s11440-014-0324-1

Where λ is the latent heat of vaporistation, R_N is the net radiation, G is the soil heat flux, $(e_s - e_a)$ represents the vapour pressure deficit of the air, ρ_a is the mean air density at constant pressure (measured on site), C_P is the specific heat of the air, Δ represents the slope of the saturation vapour pressure temperature relationship, γ is the psychrometric constant, and r_s and r_a are the (bulk) surface and aerodynamic resistances.

Net radiation was derived following the methodology outlined in Allen et al. [34] from shortwave radiation (R_S) measured on site, as was the vapour pressure deficit (calculated from humidity and temperature data). For the derivation of the aerodynamic resistance and canopy resistance, readers are directed to reference [34].

Actual evapotranspiration (ET) was calculated by scaling the PET. Its limits are defined such that at full saturation, ET=PET. When suctions develop the vegetation is less able to uptake water which reduces the water available for ET. Transpiration reaches zero at a suction of 1,500 kPa (the plant permanent wilting point) at a maximum rooting depth of 300 mm.

The surface storage term is also more complex to derive as the moisture content/suction measurement locations are within the embankment slopes so all water that would pond on the surface instead is assumed to be lost as run-off. However a tendency for water to pool at the base of the ballast at the crest of the slope has been observed, and this may recharge into the soil mass even when rainfall is not occurring until it too is exhausted. It is assumed that drainage is primarily vertical and that the impact of this ballast ponding recharge on the measurement point within the slope is negligible (due to the horizontal distance between these two locations) when compared to gravitational drainage at the point of interest and ET losses from the surface above.

Estimation of the run-off and evapotranspiration parameters requires assumptions to be made about the surface of the embankment, the vegetation cover (and hence rainfall interception, canopy water storage, the rooting depth) and how these variables may change over time. In this work, the crest is assumed to be bare of vegetation and the shoulders covered with grass 0.3 m tall. Deep percolation below the rooting zone occurs due to gravity flow and will continue as long as the soil moisture content is higher than field capacity and is assumed to take water below the level of the root water uptake zone.

The final publication is available at Springer via
http://dx.doi.org/10.1007/s11440-014-0324-1

3.3 Pore water pressure monitoring

Typically, embankments are built above the water table. The aim is to ensure that the fill material is close to the optimum water content during construction. This means that pore water pressure, at the time of construction, will be negative. However, pore water pressures will change with time, as a result of volumetric changes, shear strains, rainfall infiltration and moisture extraction by plants. As previously stated, over the period studied almost zero movements have occurred in the embankment. Therefore, all pore water pressure changes were attributed to the effects of effective recharge. All surface cracking was attributed to desiccation.

MPS-1 dielectric water potential sensors produced by Decagon Ltd were installed in December 2008 (south slope) and March 2010 (north slope) of panel A. These devices can measure soil suction in the range of −10 to −600 kPa and are accurate to 20 % of total soil suction measured. The sensors were positioned at the base, mid point and top of the slope on each aspect at depths of 0.5 and 1 m (locations shown on Figure 1) and measurements taken hourly.

3.4 Electrical resistivity tomography (ERT) characterisation and monitoring

Geoelectrical imaging techniques like ERT are now widely used for studying environmental and engineering problems, including the characterisation and monitoring of slopes. Electrical resistivity tomography produces spatial or volumetric models of subsurface resistivity distributions, from which features of contrasting or changing resistivity may be characterised or monitored. Methodologies for ERT data collection and modelling are described widely in the literature (e.g. Friedel et al. [35]; Chambers et al. [36]), so only a short summary is provided here.

Two permanent ERT monitoring arrays have been installed within the well-compacted and poorly compacted sections of the trial embankment, respectively. The electrode arrays have been installed a few centimetres below the ground surface to prevent damage to the cables. Each line comprises 64 electrodes at 0.5 m intervals, running from the toe of the northern flank to the toe of the southern flank.

Measurements have been made using an AGI Super Sting R8/IP resistivity instrument. All resistivity data were collected using the dipole–dipole array configuration, with dipole sizes (a) of 0.5, 1, 1.5, 2, 2.5, 3, 3.5 and 4 m, and unit dipole separations (n) of 1a to 8a. The dipole–dipole command sequences comprised full sets of both normal and reciprocal configurations; comparison of forward and reciprocal measurements provided a robust means of assessing data quality and determining reliable and quantitative data editing criteria. The data were inverted using the regularised least-squares

optimisation method [37], in which the forward problem was solved using the finite difference method. Data noise estimates, based on calculated reciprocal errors, were used to weight the measurements during the inversion process. Good convergence between the observed and model data was achieved, as indicated by absolute misfit errors of between 1 and 2.7 %.

Monitoring using multi-level sensors has been undertaken at the test site to determine seasonal temperature changes in the subsurface; these data have been used to correct the time-lapse ERT images for temperature effects using a methodology similar to that described by Chambers et al. [36] and Brunet et al. [38]. Seasonal temperature changes in the subsurface can be described by the following equation,

$$T(z,t) = T_{\text{mean}}(air) + \frac{A}{2} e^{-(z/d)} \sin(\omega t + \varphi - z/d) \qquad 4$$

where $T(z,t)$ is the temperature at day t and depth z, $T_{\text{mean}}(air)$ is the mean yearly air temperature, A is the yearly amplitude of the air temperature variation, d is the characteristic penetration depth of the temperature variation, φ is the phase offset, $(\phi - z/d)$ is the phase lag, and ω is the angular frequency ($2\pi/365$). The temperature data were fitted to Equation 4 using the FindMinimum[] function in the Mathematica computational algebra package. This is a Quasi-Newton method, which uses the Broyden–Fletcher–Goldfarb–Shanno algorithm to update the approximated Hessian matrix [39]. The modelled seasonal temperature variations with depth were used to correct the 2D and 3D ERT models, with the assumption that resistivity decreases by 2 % per 1 ^{o}C increase in temperature [40]. Resistivities for all ERT models were normalised to the mean air temperature (9.4 ^{o}C).

The resistivity ρ was related to moisture content using the Waxman-Smits model [41]

$$\rho_{\text{WS}} = \frac{a}{\varphi^m S^n} \left(\frac{1}{\rho_{\text{w}}} + \frac{B Q_{\text{v}}}{S} \right)^{-1} \qquad 5$$

where S is the saturation, φ is the porosity, Q_{v} is the cation concentration per unit pore volume (in meq cm^{-3}) and the remaining parameters are defined in Table 1.

The final publication is available at Springer via
http://dx.doi.org/10.1007/s11440-014-0324-1

Table 1: Waxman-Smits parameters

Parameter	Capping Layer	Notes	Embankment	Notes	Units
Tortuosity factor, *a*	1.0	Estimated	1.61	Fitted	-
Cementation exponent, *m*	1.5	Estimated	1.95	Fitted	-
Saturation exponent, *n*	2.0	Estimated	3.65	Fitted	-
Pore water resistivity, ρ_w	15.0	Estimated	15.0	Estimated	Ωm
Pore water density , P_w	1.0	-	1.0	-	g cm^{-3}
Solid density, P_s	2.4	Measured	2.65	For silica	g cm^{-3}
Average ionic mobility, *B*	1.98	Estimated	1.98	Estimated	(Sm^{-1}) cm^3 meq^{-1}
Cation exchange capacity, *C*	0	-	15.2	Measured	meq/100g

Note that the Waxman-Smits model is equivalent to Archie's Law if $Q_v = 0$. Rewriting this model in terms of the dry soil gravimetric moisture content, $G = \frac{\varphi P_w}{(1-\varphi)P_s} S$, we obtained

$$\rho_{WS} = \left(\frac{\varphi P_w}{(1-\varphi)P_s}\right)^n \frac{a}{\varphi^m G^n}\left(\frac{1}{\rho_w} + \frac{BCP_w}{100G}\right)^{-1} \qquad 6$$

where $Q_v = \frac{(1-\varphi)P_s}{\varphi}\frac{C}{100}$ has been substituted in terms of the cation exchange capacity *C*. The parameters *a*, *m*, and *n* were found by fitting equation 2 to laboratory measurements of resistivity as a function of moisture content for a representative sample of embankment material with a porosity of φ = 0.377. The fitted model is shown in Figure 6. For the capping material, *a*, *m*, and *n* were estimated to be representative values for clean sand and gravel [42].

The final publication is available at Springer via
http://dx.doi.org/10.1007/s11440-014-0324-1

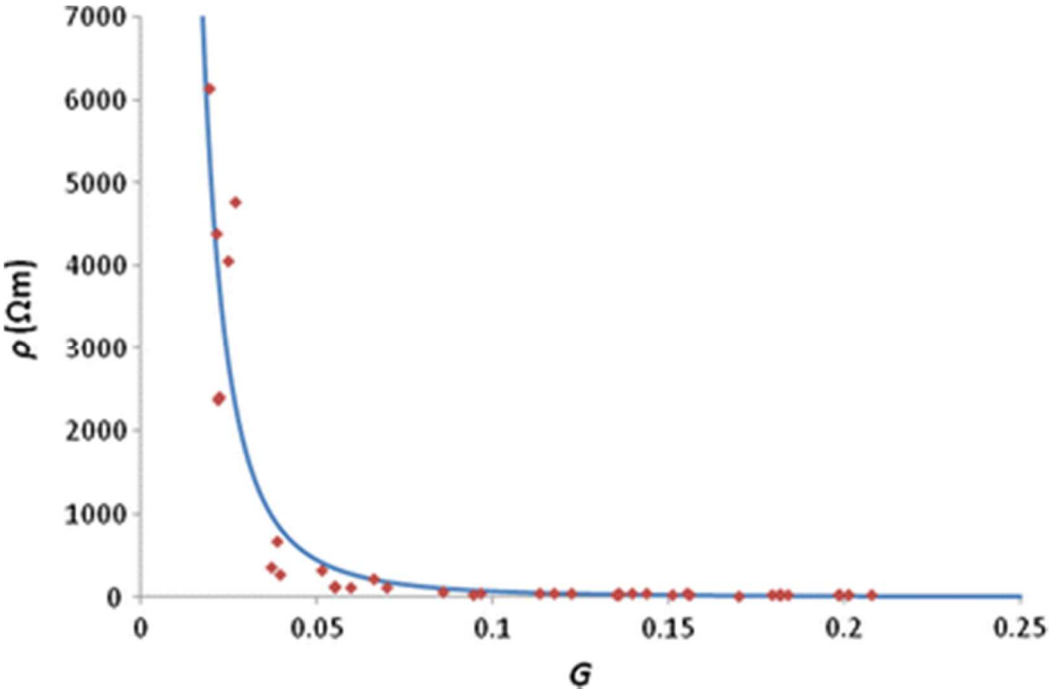

Figure 6: Waxman–Smits model fitted to laboratory measurements of resistivity versus gravimetric moisture content

The embankment was constructed in a series of layers with samples taken of every layer. The porosities of each sample were measured and are listed in descending layer order in Table 2. The porosity of the capping layer was estimated from the properties of the bulk aggregates used to construct it. With the exception of the capping layer, all the layers were assumed to have the same Waxman–Smits model parameters (other than porosity).

Table 2: Porosities of embankment layers

	Poorly compacted		Well compacted	
Layer	Thickness (m)	Porosity	Thickness (m)	Porosity
Capping	0.5	0.125	0.5	0.125
1	0.5	0.393	0.36	0.378
2	1.0	0.395	0.36	0.369
3	1.0	0.393	0.36	0.390
4	1.2	0.392	0.36	0.365
5	0.3	0.375	0.36	0.361
6	0.3	0.377	0.36	0.348
7	0.3	0.385	0.36	0.367
8	0.3	0.371	0.36	0.355
9	0.3	0.383	0.36	0.351
10	0.3	0.354	0.36	0.380
11	-		0.36	0.365
12	-		0.36	0.317
13	-		0.36	0.358
14	-		0.36	0.393
15	-		0.36	0.392
16	-		0.36	0.367

The final publication is available at Springer via
http://dx.doi.org/10.1007/s11440-014-0324-1

To apply the Waxman–Smits model, a grid of cells was constructed using the measured topography as a known reference. The vertical edges of the Waxman–Smits cells were chosen to align with those of the cells in the corresponding resistivity image. The vertical extent of each cell was equal to the layer thickness under the crest of the embankment, and the layers were tapered linearly with horizontal distance to the toes of the embankment. The resulting structure of the Waxman–Smits (a) and resistivity image (b) grids are shown in Figures 7 and 8 for the poorly and well-compacted regions of the embankment, respectively.

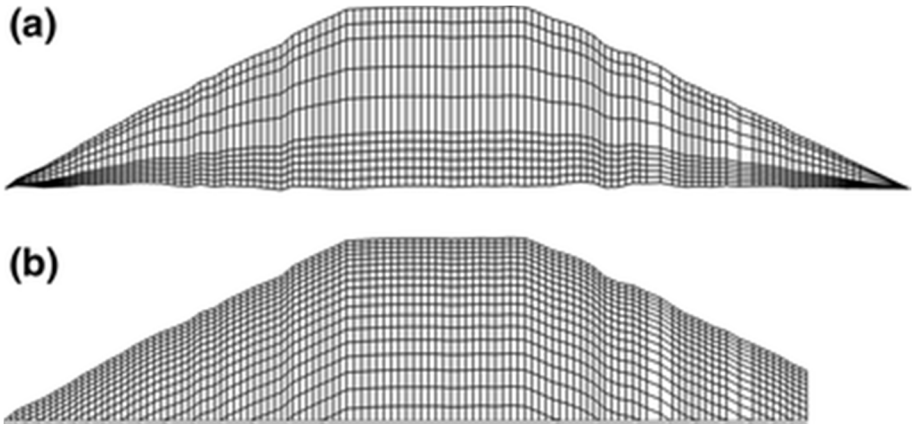

Figure 7: Poorly compacted region. (a) Waxman–Smits cells. (b) Resistivity image cells (cut-off at ground level)

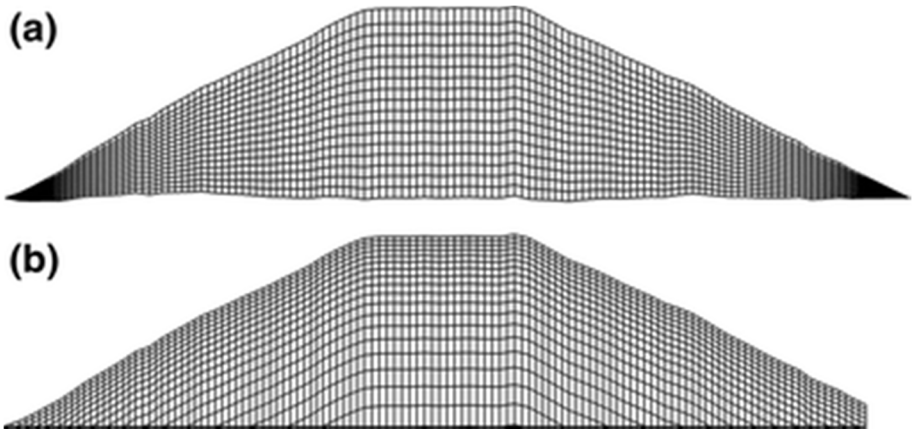

Figure 8: Well-compacted region. (a) Waxman–Smits cells. (b) Resistivity image cells (cut-off at ground level)

In order to translate the ERT images into images of moisture content, the resistivity of each ERT cell *i* was expressed as the geometric mean of the resistivities of the contributing Waxman-Smit cells *j*

The final publication is available at Springer via
http://dx.doi.org/10.1007/s11440-014-0324-1

$$\rho_i = \exp \sum_j f_{ij} \ln \rho_{\mathrm{WS}j}(G) \qquad 7$$

where f_{ij} is the area of intersection of ERT cell *i* and WS cell *j* divided by the area of ERT cell *i*, and *G* is assumed to be the same in each of the contributing WS cells (i.e. those cells for which $f_{ij} \neq 0$). Equation 6 was then solved numerically to give a value of *G* for each ERT cell.

4. Results

4.1 Permeability

Figures 9 and 10 show the results of in situ tests performed on the embankment at various depths below the ground surface. Due to the way the tests were performed, the depth represents the depth below ground surface rather than the crest surface. These tests determined that there is significant variation in permeability with depth below surface, aspect and degree of compaction. Permeability decreases with depth below surface in the zone between 0 and 1.4 m. Permeability is higher on the north slopes than on the south and is higher in poorly compacted panel A than in well-compacted panel B.

In situ permeability is orders of magnitude higher than permeability determined in the laboratory, ranging between 10^{-6} and 10^{-9} m/s in the well-compacted panel and between 10^{-5} and 10^{-9} m/s in the poorly compacted panel. In situ measurements were made during 2009, more than 3 years after construction when the effects of seasonal wetting and drying, desiccation cracking and plant roots will have clearly altered the in situ density from that measured immediately post construction, and therefore, also the permeability of the soil within the depth range tested. The advantage of in situ tests is that they can take these effects into account, although in the case of the data presented in Figures 9 and 10 readings were taken purposely at least 1 m from any large surface cracks so as to avoid the influence of very large surface features. The values recorded indicate a clear difference between the permeability of the well and poorly compacted panels, as might be predicted from the determination of the respective SWRCs.

The final publication is available at Springer via
http://dx.doi.org/10.1007/s11440-014-0324-1

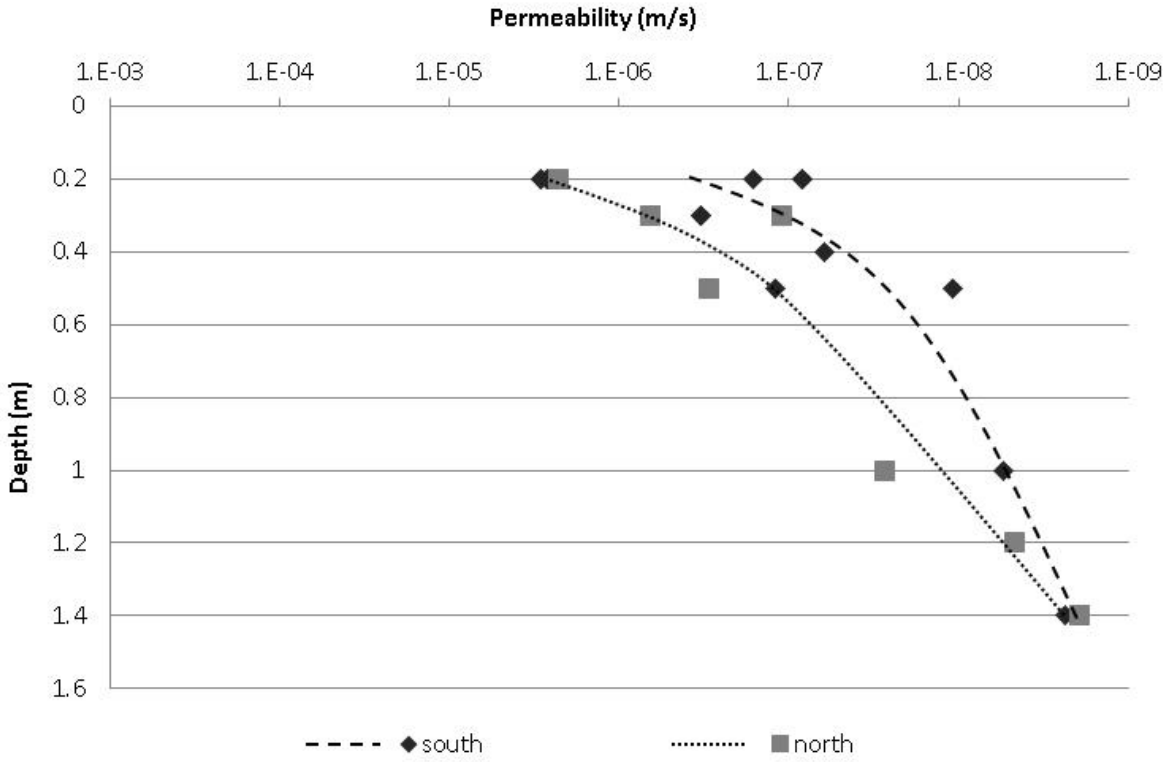

Figure 9 - Permeability of north and south aspects of panel A, tested May 2009.

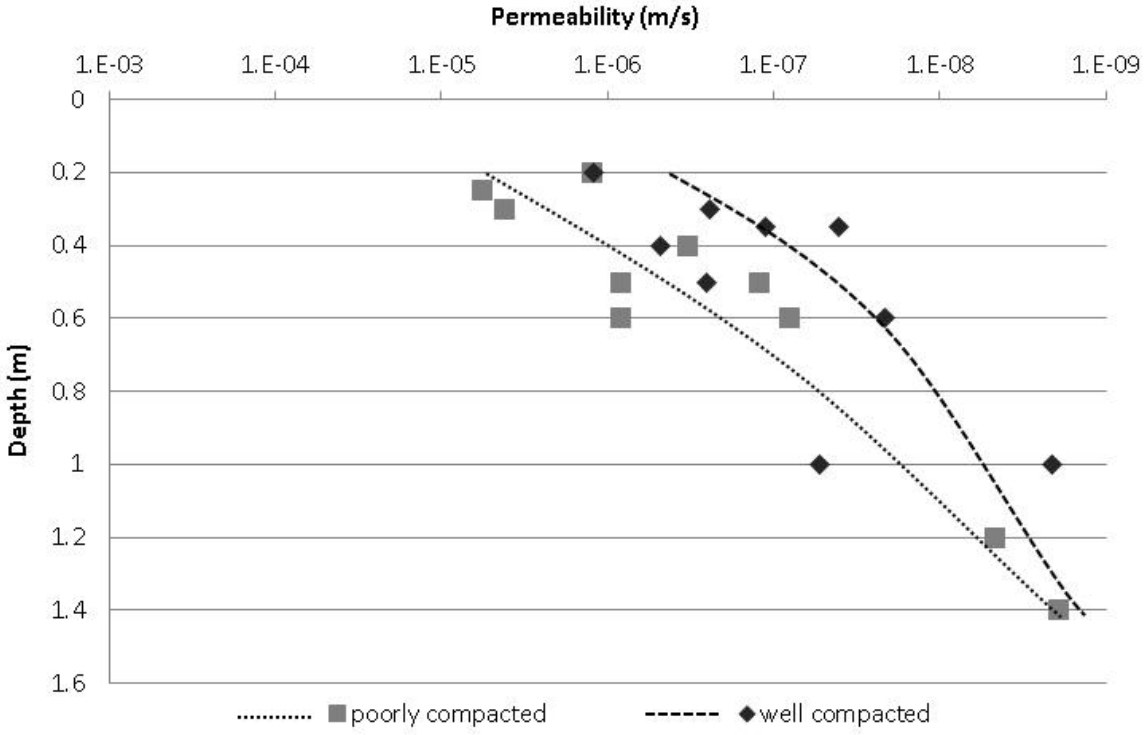

Figure 10 - Permeability of south slopes of poorly and well compacted panels, tested May 2009

The final publication is available at Springer via
http://dx.doi.org/10.1007/s11440-014-0324-1

4.2 Water balance

The resulting effective recharge (in mm/day) for the crest and the slopes of the embankment calculated by subtracting evapotranspiration and run-off derived from computer simulation from the measured precipitation are presented in Figure 11 and include a mixture of both natural and artificial rainfall.

4.3 Pore water pressure

Pore water pressure response with depth in the poorly compacted panels of the test embankment is shown in Figures 11 and 12. The results shown are taken from panels A and B where the largest number of pore pressure monitoring instruments are concentrated. Pore pressure monitoring equipment was installed beneath the south slope of panel A in December 2008 and in the north slope of panel A in March 2010.

Figure 12 shows the pore water pressure response on the north and south slope of poorly compacted panel A. The sensors used for monitoring in these zones (MPS-1s supplied by Decagon Devices) have a limited monitoring range between −10 and −600 kPa. Therefore, positive pressures could not be measured. Pore water pressures clearly responded to weather events: during relatively dry periods (periods of zero or negative effective recharge) pore water pressures can be observed to reduce progressively; during periods of high effective recharge (during imposed rainfall events) the pore water pressures rise rapidly reaching the limit of the measurement range of the sensor. Pore water pressures higher up in the slope can also be observed to respond more rapidly to weather events than those recorded close to the base.

Pore water pressures recorded at shallow depths (0.5 m) respond more rapidly to dry periods and periods of increased rainfall than those recorded at greater depths. They can also be seen to reach lower values during the drying periods (the lowest recorded values being approximately −600 kPa at 0.5 m depth and approximately −300 kPa at 1 m depth). However, this effect is less visible during the first wetting period, which can be attributed to the intensity of the rainfall.

The final publication is available at Springer via
http://dx.doi.org/10.1007/s11440-014-0324-1

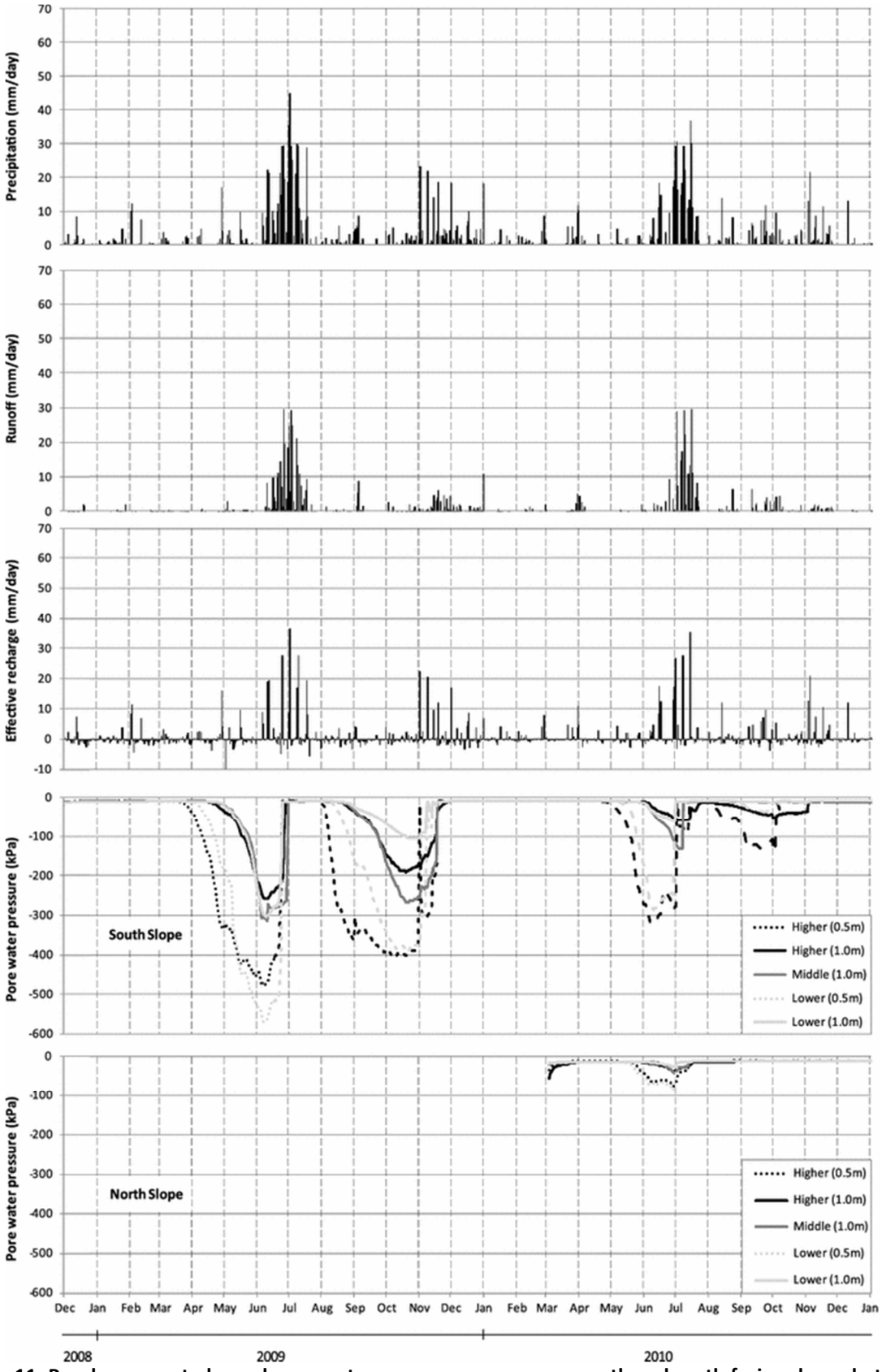

Figure 11: Poorly compacted panel pore water pressure response on south and north facing slopes between 11/2008 and 12/2010, measured using Decagon MPS1 sensors. Note Measurements taken from top, middle and base of the slope (locations shown on Figure 1). Rainfall is combination of natural and artificial (artificial rainfall periods applied in July 2009 and 2010)

The final publication is available at Springer via
http://dx.doi.org/10.1007/s11440-014-0324-1

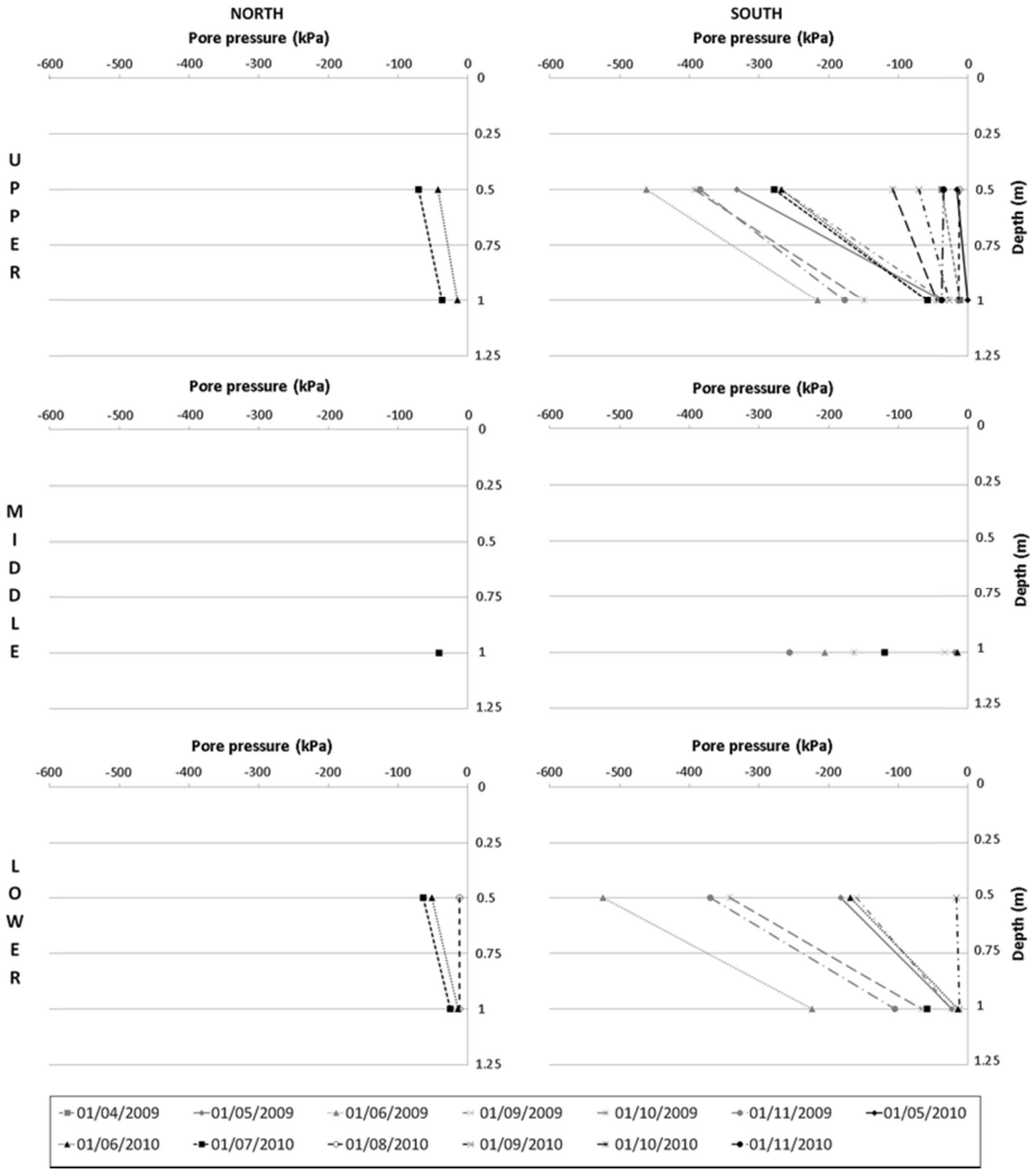

Figure 12: Pore pressure profiles beneath embankment slopes in poorly compacted panel A on north and south slopes (note at the slope mid points only one MPS-1 was installed hence the absence of data from 0.5 m depth in these plots)

Figure 12 also shows that the pore water pressures on the North Slope respond less quickly than the south slope to drying periods (they remain above the measureable range for longer). They also do not reach values as low as on the south slope (Figure 11). Averages are approximately −100 kPa at 0.5 m and approximately −50 kPa at 1 m corresponding to values of approximately −300 and −100 kPa, respectively, recorded during the same period on the south facing slope. The precipitation, run-off and effective recharge on Figure 11 show that whilst significant rainfall has occurred during the monitoring period the majority of the rainfall goes to run-off and does not infiltrate into the slope.

The final publication is available at Springer via
http://dx.doi.org/10.1007/s11440-014-0324-1

4.4 Resistivity

Clearly, there was a significant difference between the water movement and hence the permeability between the well- and poorly compacted panels. However, it was not possible to determine a definitive relationship between density and permeability from the data gathered from laboratory testing of specimens prepared from the field, or field testing. This was because density was measured on a small number of discrete samples taken during construction at heights determined above the foundation, whereas permeability was measured in situ at depths below ground surface. Furthermore, the effects of desiccation and plant rooting had altered the density from that measured immediately after construction (discussed in Section 5.3). Therefore, resistivity surveys were conducted through panel A and panel B in order to gain a holistic understanding of moisture content changes throughout the embankment cross section.

Resistivity surveys were performed in June 2010 and April 2011, the results of which are shown in Figure 13. The high resistivity of the embankment capping material is easy to identify as is the low resistivity zone in the core of the embankment, particularly in the poorly compacted panel and beneath the capping layers in both panels. Beneath the slopes of the embankment, it can be seen that the near-surface material has a relatively low resistivity (and correspondingly a low water content). On this basis, the resistivity survey can be taken as evidence that the slopes and the core of the embankment are significantly drier than the material immediately beneath the crest.

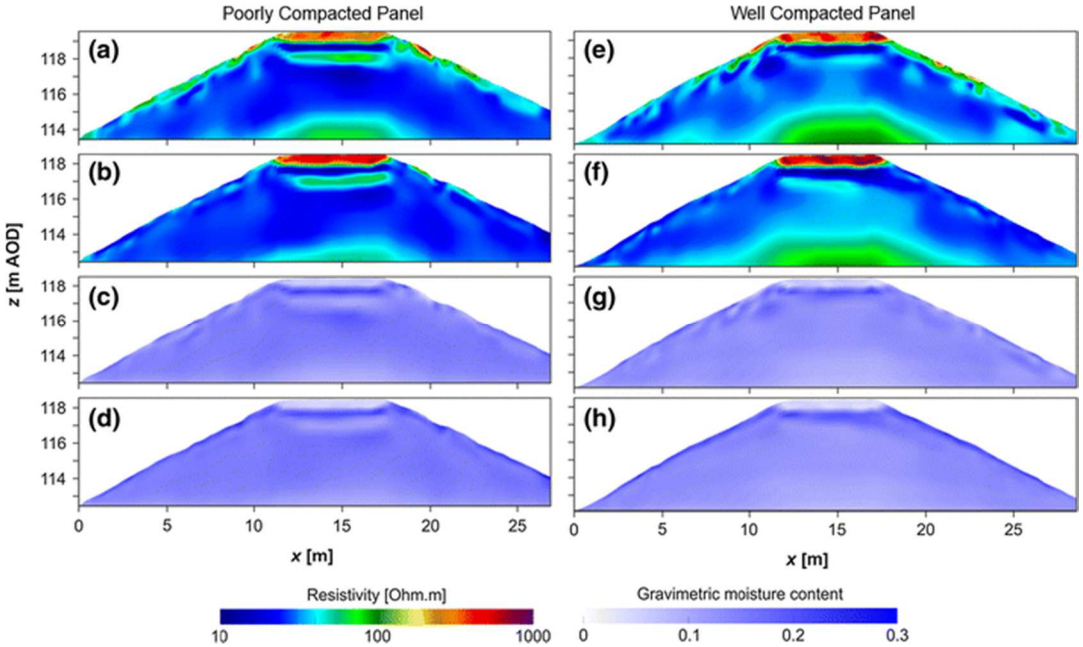

Figure 13: Uncompacted section: (a) June 2010 resistivity, (b) April 2011 ERT resistivity, (c) June 2010 gravimetric moisture, (d) April 2011 gravimetric moisture content. Compacted section: (e) June 2010 resistivity, (f) April 2011 ERT resistivity, (g) June 2010 gravimetric moisture, (h) April 2011 gravimetric moisture content. In all sections right side = southern shoulder, left side = northern shoulder

The final publication is available at Springer via
http://dx.doi.org/10.1007/s11440-014-0324-1

5. Discussion

The data presented in this paper show that pore water pressure response of a clay embankment to weather events is strongly influenced by permeability and soil water retention behaviour, which are intrinsically linked to particle size distribution and degree of compaction. Poor compaction leads to higher permeability which leads to a more rapid pore water response and poor compaction leads to a lower air-entry value which leads to less summer suction for the same change in water content. The response is also influenced by slope aspect which in turn influences the weather events to which the embankment is subjected. There are, therefore, complex interactions which need to be unpicked and potentially significant implications for the ongoing management of infrastructure slopes.

5.1 Compaction

The observed difference in soil water retention behaviour between poorly compacted and well-compacted field specimens can be attributed to the difference in fabric (i.e. pore distribution) that the different levels of compaction impart upon the same base material. This in turn controls permeability at the microscale. The poorly compacted material has a higher volume of voids than the well-compacted material. Hence, the saturated permeability of the poorly compacted material is higher than that of the well-compacted material, as might be predicted. However, the degree of saturation is not constant, as demonstrated by pore pressure measurements shown in Figures 11 and 12. The soil water retention behaviour for the different levels of compaction has also been shown to vary (Figure 4). Therefore, the transient permeability; the changing permeability due to its degree of saturation, is also different for the different levels of compaction. The implication is that there is a twofold impact of poor compaction on permeability and hence pore water pressures in embankment slopes (i.e. poor compaction leads to higher permeability and a greater degree of fluctuation in permeability with degree of saturation and hence with time). The greater variability in pore pressure caused by these differences also has implications for potentially increased shrink swell behaviour in poorly compacted embankments (particularly those constructed from higher plasticity material than in our test embankment) and hence higher maintenance costs.

This has implications for the relative maintenance of road versus rail embankments. Not only do railway embankments suffer due to ingress of water and shrink–swell due to poor compaction, they may also suffer greater fluctuations in permeability, causing even greater shrink–swell cycles and faster rates of ageing. Therefore, compaction is important not just to reduce permeability in the short term but to prevent the type of pore pressure fluctuation or cycles that can lead to the early onset of progressive failure.

The final publication is available at Springer via
http://dx.doi.org/10.1007/s11440-014-0324-1

5.2 Micro- and macroscale effects

Saturated permeability, when measured at the microscale, was consistently lower in the south aspect than in the north, as demonstrated in Figure 9. The in situ permeability was measured at the end of a dry period when suctions were at their highest and would have the greatest potential to affect the in situ permeability. Whilst the Guelph Permeameter measures steady state and hence saturated permeability, it is believed that there would be some influence of zones or peds that would have remained partially saturated. Measurements were made in areas where there was no evidence of surface cracking which would have influenced the values recorded. However, the increased drying on the southern aspect had caused a larger number of desiccation cracks to form, as well as an increase in crack size, so if measurements had been taken adjacent to areas where cracking was present, then the values recorded would be higher than those presented in this study.

One clear implication of the variable nature of the fill material is with regard to the soil water retention behaviour whereby macro (pore) features like desiccation cracks will desaturate more rapidly at much lower suctions than the soil micro (pore) matrix, whereby the suctions generated are a function of the pore (or void/crack) widths and capillary tension forces. This suggests that traditional single-porosity SWRC models [43, 44] will not capture the in situ SWRC of a cracked soil and instead it would be necessary to account for this behaviour using some form of dual-porosity model such as that proposed by Durner [45] or by Fredlund et al. [46].

Work by Springman et al. [47] has also identified the importance of both micro- and macroscale features on permeability and the implications for slope stability at field scale, and other work has identified the importance of dual-porosity features on water retention behaviour [48, 49]. Preliminary investigations of the in situ soil water retention behaviour (shown in Figure 14) derived for the embankment shoulders at a depth of 0.5 m suggests that there is dual-porosity behaviour within the embankment fill with a reduction in the rate of desaturation occurring at suctions from 100 to 200 kPa. Furthermore, and perhaps more significantly, the SWRC behaviour has changed over time, with near-surface weathering effects being a possible explanation.

The final publication is available at Springer via
http://dx.doi.org/10.1007/s11440-014-0324-1

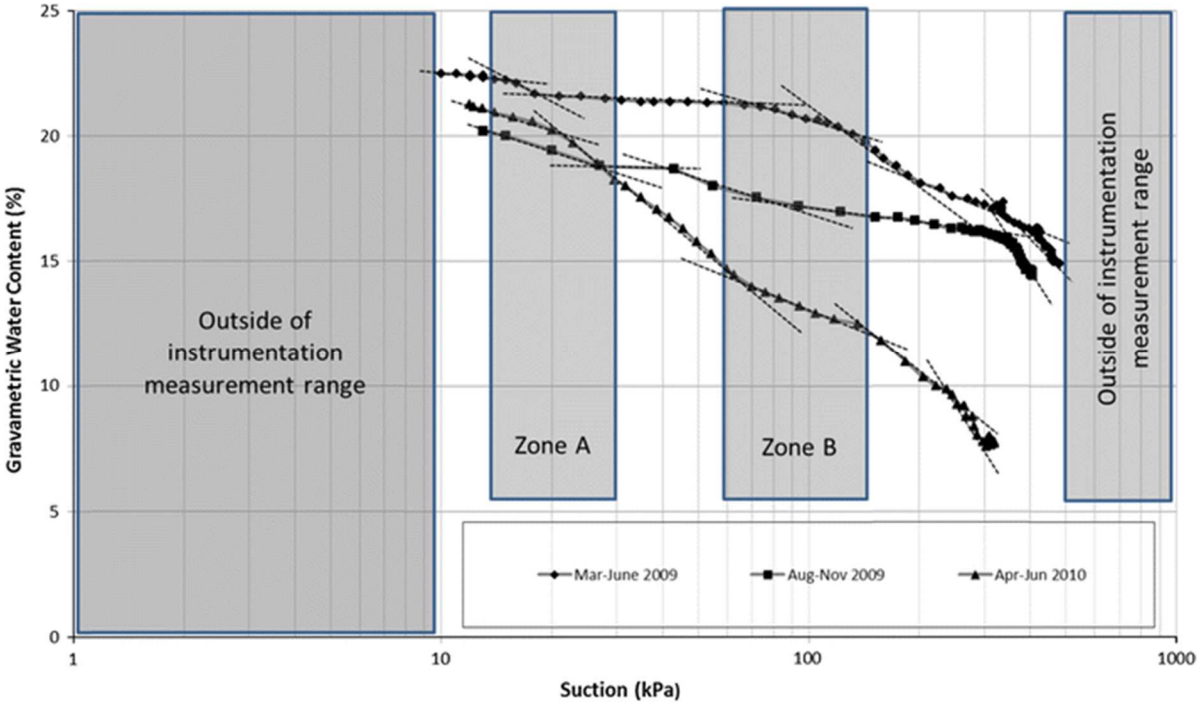

Figure 14: In situ soil water retention curves measured using dielectric water potential sensors located on the south aspect of poorly compacted panel A

5.3 Development of a 'near surface zone'

The permeability, pore water pressure and resistivity monitoring all show that the major changes within the embankment are occurring between 0 and approximately 1.4–1.5 m depth in the near-surface zone. Permeability changes by up to 4 orders of magnitude within this range, and this is where the most significant pore water pressure variations occur. At depths lower than 1.4 m, permeability and pore water pressures are more consistent. This zone also corresponds with the vegetation root zone as noted during the excavation of observation pits.

Understanding the processes that control pore pressures and permeability within the near-surface zone is therefore crucial to predict the stability of embankments, especially in response to weather events.

The transient nature of permeability and pore water pressure in this near-surface zone means that this region is more likely to reduce in strength over time and maintenance regimes should specifically target observations in this zone. Measurement of density with depth immediately post construction for both well- and poorly compacted panels is shown in Figure 3a. It shows no distinct change in density at a depth of around 1.5 m, which means that the 'near surface zone' probably develops with time after construction due to the action of vegetation and shrink–swell of the clay. It is not yet clear whether this zone will penetrate to greater depths with increasing time or with greater seasonal

variation in climate. However, it is interesting to note that other authors [22] also observed a distinct difference in soil water response below 1.5 m which they attributed to density changes.

5.4 Aspect

The pore water pressure differences between the north and south aspect of the embankment during dry periods can be attributed to differences in local climate due to the orientation of the slopes. The different conditions on each aspect also promote the growth of different types of vegetation [9] which further exacerbates these differences. During the study period, the south aspect received more sunlight, had more actively growing vegetation and was exposed to wind from a southerly direction. This induced a greater amount of evapotranspiration, greater drying and hence higher soil suctions on the south slope. Standard methods of calculating evapotranspiration are not capable of capturing these differences between aspects as weather data is taken from the nearest available weather station in most cases, often some distance from the site under investigation, and differences in weather between the different aspects would not be taken into account. It should be straightforward to predict which aspect of an embankment would be expected to experience a greater degree of drying, however, because a significant amount of drying is caused by wind. There is the potential for this to change over time if the prevailing wind direction changes, either due to natural climatic variation or the removal of a natural wind break.

When assessing embankment stability, practitioners should consider the effects of aspect. This may include modelling each individual aspect/slope separately and/or obtaining site-specific weather data for each aspect. Typical numerical modelling methods in which only one half of an embankment slope is modelled will not capture differences between slopes and may not be able to identify the most vulnerable areas. Additionally, different aspects may need different routine observation, with northerly facing slopes which are away from the prevailing wind tending to be wetter and needing more attention in prolonged wet periods and southerly facing slopes in the prevailing wind tending to crack in periods of extended drying.

5.5 Effective stress and deformation

The suctions developed in the southern shoulder of the embankment (ranging from approx. 120–550 kPa, see Figure 11), and their dissipation during periods of wetter weather lead to large fluctuations in the effective stress at these locations which in turn will lead to significant changes in shear strength. However, to date, there is no evidence within this trial embankment of these fluctuations leading to settlements or the development of shear or volumetric strains at any point

The final publication is available at Springer via
http://dx.doi.org/10.1007/s11440-014-0324-1

within the slope. Further to this, there is in turn no evidence of shrink swell behaviour which may lead to strain softening or down slope ratcheting of the type posited by Leroueil [13] and Take and Bolton [50] as potential slope failure mechanisms during climate cycling. This means that as there has been very little movement within the embankment to date. For the purposes of this full-scale experiment, the generated pore water pressures have been assumed to be the result of meteorological variations alone.

5.6 Surface capping of the embankment crest

The nearly saturated conditions indicated beneath the crest by the resistivity surveys are almost certainly caused by ponding of water at the base of the granular capping layer above the compacted fill, causing the material beneath to remain saturated throughout the year. This is compounded by the low levels of run-off from the crest due to the higher permeability of the granular capping layer. This is most pronounced in the well-compacted layers where the lower permeability tends to increase ponding and hence maintain higher pore water pressures in this region over the longer term. By contrast, this material is not present on the shoulders of the embankment which are instead vegetated. Hence, there is greater potential for evapotranspiration, and there is less infiltration due to higher levels of run-off caused by the slope angle. These results are similar to those reported by Ridley et al. [2].

The implications for rail embankments are clear, where the ballast beneath the tracks will respond in the same way as the capping layer, causing ponding beneath the crest. This has been reported by many authors, including Perry et al. [1]. The implications for road embankments are less clear, particularly, because the embankment does not fully simulate the hydraulic boundary conditions due to the presence of the capping layer. It may be that the relatively impermeable surfacing will prevent high pore water pressures from developing beneath the crest, and good maintenance of drainage will be required to ensure that run-off does not cause greater problems on the shoulders.

6. Conclusions and significance

The major conclusions from the work presented herein that are of significance to both researchers and practitioners in this field:

- Pore water pressure responses of clay embankments to weather events are most pronounced in the near surface (0 m to approximately 1.5 m from ground surface);
- Degree of compaction influences both the baseline microscale permeability of embankment fill and the extent to which it changes due to varying degree of saturation induced by weather events. We have demonstrated that any future modelling of long-term pore water pressure behaviour should take the transient permeability into account. This also has wider significance in that older, poorly compacted embankments are deteriorating at a faster rate than newer earthworks constructed in accordance with modern construction standards. This highlights the necessity for new earthworks to be constructed to rigorous compaction standards not merely to achieve desired strength and stiffness but also to reduce the rate of deterioration in response to weather events.
- Slope aspect has a strong influence on both degree of saturation (and hence microscale permeability), evapotranspiration and evaporation and hence strongly influences pore water pressure responses during climatic events. Hence, this work has shown for the first time that there is a need to treat different aspects as different slopes, to be modelled, monitored and maintained as different entities. Treating road and rail infrastructure corridors (or even discrete lengths of corridor) as single embankment entities, having similar management and maintenance requirements, on both faces could lead to the inability to anticipate failures and incur higher costs through the necessity to repair ultimate limit state failures rather than manage and maintain the asset.
- Differences in capping layer material and relative degree of compaction mean that road and rail embankments are likely to have different pore water pressure regimes and behave differently during climatic events. Therefore, lessons learned from one sector should only be transferred to another with a degree of caution; and
- A near-surface zone of approximately 1.4–1.5 m in depth from the surface develops with time after construction, in which transient behaviour and the effects of macro features are most pronounced. This work has added further evidence to the body of research which shows that this zone is key to understanding both the overall stability of an embankment, and also its ongoing monitoring, and maintenance requirements. It is vitally important that future research is undertaken to improve the understanding of the science underpinning the development of this zone and its engineering implications.

The final publication is available at Springer via
http://dx.doi.org/10.1007/s11440-014-0324-1

Acknowledgments

The authors wish to acknowledge funding for the BIONICS project from the Engineering and Physical Sciences Research Council (BIONICS GR/S87430/01) and also continued funding from the EPSRC Platform Grant in Earth Systems Engineering (EP/G01343/1), iSMART (EP/K027050/1), the BGS British University Funding Initiative and COST TU1202. They would also like to thank the industrial sponsors to the research including Network Rail, the Highways Agency, Mott Macdonald, London Underground and Geo-Observations Ltd. The input from the other academic partners for the Universities of Dundee, Durham, Loughborough, Nottingham Trent and Bristol are also gratefully acknowledged. The contributions of J.E. Chambers, P.B. Wilkinson and D.A. Gunn are published with the permission of the Executive Director of the British Geological Survey, NERC. Researchers wishing to make use of the raw datasets used in the preparation of this paper are invited to contact the authors.

7. References

[1] Perry J, Pedley M, Reid M (2001). *Infrastructure Embankments: Condition Appraisal and Remedial Treatment*. CIRIA, London, Report C550.

[2] Ridley A, Mcginnity B, Vaughan PR (2004). Role of pore water pressures in embankment stability. *Proceedings of the Institution of Civil Engineers, Geotechnical Engineering* **157**:193–198.

[3] Glendinning S, Hall J, Manning L, (2009a). Asset-management strategies for infrastructure embankments. *Proceedings of the Institution of Civil Engineers, Engineering Sustainability* **162**:111–120.

[4] Anderson M.G, Kneale PE (1982). The influence of shrinkage cracks on pore pressures within a clay embankment. *Quarterly Journal of Engineering Geology & Hydrogeology* **15**:9–14.

[5] Ridley AM, Dineen K, Burland JB, Vaughan PR (2003). Soil matrix suction: some examples of its measurement and application in geotechnical engineering. *Proceedings of the Institution of Civil Engineers, Géotechnique* **53**:241–253.

[6] Nyambayo VP, Potts DM, Addenbrooke TI (2004). The influence of permeability on the stability of embankments experiencing seasonal cyclic pore water pressure changes. *Advances in Geotechnical Engineering: Proceedings of the Skempton Conference* (JARDINE RJ, POTTS DM, HIGGINS KG (eds)). Thomas Telford, London, 2,898–2,910.

[7] Smethurst J, Clarke D, Powrie W (2006). Seasonal changes in pore water pressure in a grass covered cut slope in London Clay. *Proceedings of the Institution of Civil Engineers, Géotechnique* **56**:523–537.

[8] Hughes PN, Glendinning S, Mendes J, Parkin G, Toll DG, Gallipoli D, Miller P (2009). Full-scale testing to assess climate effects on embankments. *Proceedings of the Institution of Civil Engineers, Engineering Sustainability* **162**:67-79.

[9] Glendinning S, Loveridge F, Starr–Keddle RE, Bransby M.F, Hughes PN. (2009b). Role of vegetation in sustainability of infrastructure slopes. *Proceedings of the Institution of Civil Engineers, Engineering Sustainability* **162**:101–110.

[10] Anderson MG, Kneale PE (1980). Pore water pressure and stability conditions on a motorway embankment. *Earth Surface Processes* **5**:37–46.

[11] Skempton AW (1985). Residual strength of clays in landslides, folded strata and the laboratory. *Proceedings of the Institution of Civil Engineers, Géotechnique* **35**:3–18.

[12] Vaughan PR, Hight DW, Sodha VG, Walbancke HJ (1978). Factors controlling the stability of clay fills in Britain. *Proceedings of a Conference on Clay Fills*. Thomas Telford, London, pp. 205–217.

[13] Leroueil S (2001). Natural slopes and cuts: movement and failure mechanisms. *Proceedings of the Institution of Civil Engineers, Géotechnique* **51**:197–243.

[14] Brooks SM, Crozier MJ, Glade TW, Anderson MG (2004). Towards establishing climatic thresholds for slope instability: use of a physically-based combined soil hydrology–slope stability model. *Pure and Applied Geophysics* **161**:881–905.

[15] O'Brien AS (2007). Rehabilitation of urban railway embankments: research, analysis and stabilization. *Proceedings of the 14th European Conference on Soil Mechanics and Geotechnical Engineering*; Madrid. p. 125-43.

[16] Hudacsek P, Bransby MF, Hallett PD, Bengough AG (2009). Centrifuge modelling of climate effects on clay embankments. *Proceedings of the Institution of Civil Engineers, Engineering Sustainability* **162**:91–100.

[17] Kovacevic K, Potts DM, Vaughan PR (2001). Progressive failure in clay embankments due to seasonal climate changes. *Proceedings of the 5th International Conference on Soil Mechanics and Geotechnical Engineering*, Istanbul, **3**, 2127–2130.

[18] O'Brien A (2004). Old railway embankment clay fill: laboratory experiments, numerical modelling and field behaviour. *Advances in Geotechnical Engineering: Proceedings of the Skempton Conference* (JARDINE RJ, POTTS DM. and HIGGINS KG (eds)). Thomas Telford, London, **2**, 911–921.

[19] Scott J, Loveridge F, O'Brien AS (2007). Influence of climate and vegetation on railway embankments. *Proc. ECSMGE*, Madrid: 659-664.

[20] Rouainia M, Davies O, O'Brien T, Glendinning S (2009). Numerical modelling of climate effects on slope stability. *Proceedings of the Institution of Civil Engineers, Engineering Sustainability* **162**:81–89.

[21] Evangelista A, Nicotera MV, Papa R, Urciuoli G (2008). Field investigation on triggering mechanisms of fast landslides in unsaturated pyroclastic soils. In: Unsaturated Soils: Advances in Geo-Engineering. 1st European Conference on Unsaturated soil. Durham, UK. 2-4 July 2008. (pp. 909-915). LONDON: Taylor & Francis Group plc (UK).

[22] Ng CWW, Zhan LT, Bao CG, Fredlund DG, Gong BW (2003). Performance of an unsaturated expansive soil slope subjected to artificial rainfall infiltration. *Proceedings of the Institution of Civil Engineers, Géotechnique* **53**:143-157.

[23] Highways Agency (2009). Specification for highway works. HM Stationary Office, London.

[24] British Standard Institute (1990). *BS 1377-4: Methods of test for Soils of civil engineering purposes Part 4: Compaction-related tests*, BSI, Milton Keynes.

[25] Bulut R, Lytton R, Wray W (2001). *Suction measurements by filter paper method*. ASCE Geotechnical Special Publication No.115 pp 243-261.

[26] Leong EC, He L, Rahardjo H (2002). Factors Affecting the Filter Paper Method for Total and Matric Suction Measurements. *Geotechnical Testing Journal* **25**:321-332.

[27] Lourenço SDN, Gallipoli D, Toll DG, Evans FD (2006). Development of a commercial tensiometer for triaxial testing of unsaturated soils. In *Fourth International Conference on Unsaturated Soils, Carefree – Arizona – USA, Geotech Spec Pub No. 14*., Reston: ASCE, Vol.**2**, pp. 1875-1886.

[28] British Standard Institute (1990). *BS 1377-5: Methods of test for Soils of civil engineering purposes Part 5: Compressibility, permeability and durability tests*, BSI, Milton Keynes.

[29] Hughes P, Glendinning S, and Mendes J (2007). Construction Testing and Instrumentation of an infrastructure testing embankment, *Proceedings of the Expert Symposium on Climate Change: Modelling, Impacts & Adaptations*, Singapore, pp. 159-166.

[30] Soilmoisture Equipment Corp (2008). *Model 2800K1 Guelph Permeameter operating instructions*. Website http://www.soilmoisture.com

[31] Tindall JA, Kunkel JR, Anderson DE (1999). *Unsaturated zone hydrology for scientists and engineers*. Prentice-Hall, New Jersey.

[32] Ewen J, Parkin G, O'Connell PE (2000). SHETRAN: a coupled surface/subsurface modelling system for 3D water flow and sediment and solute transport in river basins. *ASCE J Hydrologic Eng* **5**:250-258.

[33] Monteith JL (1965). Evaporation and environment. *In: Symposium of the Society for Experimental Biology, The State and Movement of Water in Living Organisms* (GE Fogg (ed.)), Vol. **19**, Academic Press, Inc., NY. pp. 205-234.

[34] Allen RG, Pereira LS, Raes D, Smith M, *Crop evapotranspiration - Guidelines for computing crop water requirements*, Food and Agricultural Organisation of the UN, Irrigation and drainage, 1998, Report 56.

[35] Friedel S, Thielen A, Springman SM (2006). Investigation of a slope endangered by rainfall-induced landslides using 3D resistivity tomography and geotechnical testing. *Journal of Applied Geophysics* **60**:100-114.

[36] Chambers JE, Gunn DA, Wilkinson PB, Meldrum PI, Haslam E, Holyoake S, Kirkham M, Kuras O, Merritt A, Wragg J (2013). 4D Electrical Resistivity Tomography monitoring of soil moisture dynamics in an operational railway embankment. *Near Surface Geophysics*, doi:10.3997/1873-0604.2013002

[37] Loke MH, Barker RD (1995). Least-Squares Deconvolution of Apparent Resistivity Pseudosections. *Geophysics* **60**:1682-1690.

[38] Brunet P, Clement R, Bouvier C (2010). Monitoring soil water content and deficit using Electrical Resistivity Tomography (ERT) - A case study in the Cevennes area, France. *Journal of Hydrology* **380**:146-153.

[39] Press WH, Teukolsky SA, Vetterling, WT, Flannery BP (1992). *Numerical Recipes in C: The Art of Scientific Computing*, 2nd edition, Cambridge University Press, Cambridge.

[40] Hayley K, Bentley LR, Gharibi M, Nightingale M (2007). Low temperature dependence of electrical resistivity: Implications for near surface geophysical monitoring. *Geophysics Research Letters* **34**:L18402.

[41] Waxman MH, Smits LJM (1968). Electrical conduction in oil-bearing sands. *Society of Petroleum Engineers Journal* **8**:107-122.

[42] Telford WM, Geldart LP, Sheriff RE (1990). *Applied geophysics*. Cambridge University Press, Cambridge.

[43] van Genuchten M.Th (1980). A closed-form equation for predicting the hydraulic conductivity of unsaturated soils. *Soil Science Society of America Journal* **44**:892–898.

[44] Fredlund DG, Xing A (1994). Equations for the soil-water characteristic curve. *Canadian Geotechnical Journal* **31**:521-532.

[45] Durner W (1994). Hydraulic conductivity estimation for soils with heterogeneous pore structure. *Water Resources Research* **30**:211–223.

[46] Fredlund DG, Houston SL, Nguyen Q, Fredlund MD (2010). Moisture Movement Through Cracked Clay Soil Profiles. *Geotechnical and Geological Engineering* **28**:865-888.

[47] Springman SM, Askarinejad A, Casini F, Friedel S, Kienzler P, Teysseire P, Thielen A (2012). Lessons learnt from field tests in some potentially unstable slopes in Switzerland. *Acta Slovenica Geotechnica* **1**:5-29.

[48] Casini F, Vaunat J, Romero E, Desideri A (2012). Consequences on water retention properties of double-porosity features in a compacted silt, *Acta Geotechnica* **7**:139-150.

[49] Hall MR, Mooney SJ, Sturrock C, Matelloni P, Rigby SP (2013). An approach to characterisation of multi-scale pore geometry and correlation with moisture storage and transport coefficients in cement-stabilised soils, *Acta Geotechnica* **8**:67-79.

[50] Take WA, Bolton MD (2011). Seasonal ratcheting and softening in clay slopes, leading to first-time failure. *Proceedings of the Institution of Civil Engineers, Géotechnique* **61**:757–769.